

V-Loop: Visual Logical Loop Verification for Hallucination Detection in Medical Visual Question Answering

Mengyuan Jin* Zehui Liao* Yong Xia[✉]

Northwestern Polytechnical University

Xi'an 710072, China

{myjin, merrical}@mail.nwpu.edu.cn, yxia@nwpu.edu.cn

Abstract

*Multimodal Large Language Models (MLLMs) have shown remarkable capability in assisting disease diagnosis in medical visual question answering (VQA). However, their outputs remain vulnerable to hallucinations (i.e., responses that contradict visual facts), posing significant risks in high-stakes medical scenarios. Recent introspective detection methods, particularly uncertainty-based approaches, offer computational efficiency but are fundamentally indirect, as they estimate predictive uncertainty for an image–question pair rather than verifying the factual correctness of a specific answer. To address this limitation, we propose **Visual Logical Loop Verification (V-Loop)**, a training-free and plug-and-play framework for hallucination detection in medical VQA. V-Loop introduces a bidirectional reasoning process that forms a visually grounded logical loop to verify factual correctness. Given an input, the MLLM produces an answer for the primary input pair. V-Loop extracts semantic units from the primary QA pair, generates a verification question by conditioning on the answer unit to re-query the question unit, and enforces visual attention consistency to ensure answering both primary question and verification question rely on the same image evidence. If the verification answer matches the expected semantic content, the logical loop closes, indicating factual grounding; otherwise, the primary answer is flagged as hallucinated. Extensive experiments on multiple medical VQA benchmarks and MLLMs show that V-Loop consistently outperforms existing introspective methods, remains highly efficient, and further boosts uncertainty-based approaches when used in combination.*

1. Introduction

Multimodal Large Language Models (MLLMs) [7, 9, 20, 34, 40] have shown strong capabilities in medical image un-

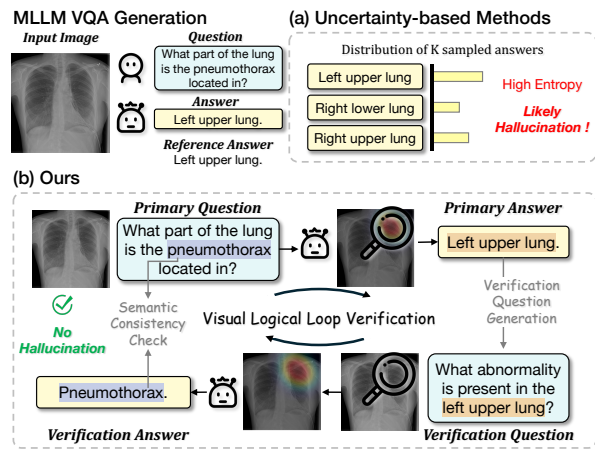


Figure 1. Comparison between uncertainty-based detection method and our proposed V-Loop. (a) Uncertainty-based methods detect hallucinations by sampling multiple answers and estimating semantic entropy. (b) V-Loop instead verifies the factual correctness of a specific answer through visual logical loop verification.

derstanding, integrating lesion recognition, severity assessment, and diagnostic reasoning within a unified framework. In medical visual question answering (VQA), they serve as promising clinical assistants that generate context-aware answers from image–question pairs. However, despite their impressive reasoning ability, medical MLLMs remain susceptible to *hallucinations*, i.e., responses that contradict the visual facts grounded in the image [5, 27]. In high-stakes clinical scenarios, hallucinated outputs can lead to misdiagnosis and loss of clinician trust, underscoring the urgent need for reliable hallucination detection [18, 37, 46].

Existing hallucination detection methods can be broadly categorized by their external dependency. **Collaborative approaches** [8, 10, 39] rely on auxiliary models or curated knowledge bases to verify generated answers, or they train dedicated detectors on carefully annotated hallucination data. While effective, their reliance on high-quality external

*Equal Contribution [✉]Corresponding Author

resources limits generalization and scalability. In contrast, **introspective approaches** [6, 14, 41] operate solely within the MLLM, inferring hallucinations by estimating models’ predictive uncertainty. As illustrated in Fig. 1, these methods, such as Semantic Entropy (SE) [14] and VASE [22], assume that higher predictive entropy indicates a greater likelihood of hallucination. This paradigm is computationally efficient but remains indirect, as it assesses model uncertainty over an input image–question pair rather than verifying the factual correctness of a specific answer.

In real-world clinical practice, a lightweight, self-contained mechanism that internally verifies each generated answer is more deployable than resource-dependent or sampling-intensive methods. Motivated by this gap, we propose **Visual Logical Loop Verification (V-Loop)**, a training-free and plug-and-play framework for hallucination detection in medical VQA. V-Loop introduces a bidirectional reasoning process that constructs a visually grounded logical loop to assess factual consistency (see Fig. 1). Given an image–question pair, the MLLM generates a *primary answer* while recording its visual attention map. From this pair, two key semantic units (one from the question and one from the answer) are extracted to form the basis of verification. A *verification question* is then constructed by conditioning on the answer’s semantic unit to re-query the question’s semantic unit, and the model is prompted to respond using the same visual evidence. If the verification answer semantically aligns with the expected content, the loop is closed, indicating that the original answer is visually grounded; otherwise, it is flagged as hallucinated. To further ensure that verification reasoning is grounded in the same visual evidence as primary reasoning, V-Loop enforces *visual attention consistency* by requiring the MLLM to reuse its primary visual attention pattern when answering the verification question.

V-Loop offers three key advantages: (1) it is **training-free and model-agnostic**, requiring no additional supervision or retraining; (2) it performs **visual-grounded self-verification** in a single step, avoiding multi-sample uncertainty estimation; and (3) it achieves **strong generalization** across diverse MLLMs and datasets. Extensive experiments on three medical VQA benchmarks and three MLLMs demonstrate that V-Loop consistently outperforms existing introspective and uncertainty-based methods.

The main contributions of this work are threefold:

1. We propose *V-Loop*, a training-free, plug-and-play hallucination detection framework that verifies the factual correctness of medical VQA responses.
2. We design a *visual logical loop verification mechanism* that verifies consistency between the model’s bidirectional reasoning steps while maintaining *visual attention consistency* between primary and verification stages.
3. Comprehensive evaluations on three medical VQA

benchmarks and three MLLMs show that V-Loop consistently outperforms competing methods and further improves uncertainty-based approaches when combined.

2. Related Work

2.1. Medical VQA

Medical VQA aims to generate clinically meaningful answers to image–question pairs [13, 24]. With the emergence of MLLMs [2, 4, 26, 45], medical adaptations [3, 7, 20, 34, 40] have demonstrated remarkable progress in clinical image understanding through instruction tuning and domain-specific alignment. Despite these advances, hallucinations remain prevalent, as MLLMs often produce responses that deviate from visual evidence or clinical facts.

To evaluate the reliability of generated answers, traditional text similarity metrics such as BLEU [31], ROUGE [23], and BERTScore [44] primarily measure lexical overlap and fail to capture factual correctness or clinical semantics. To address this limitation, concept-aware metrics such as CHAIR [32] and CBSS [35] incorporate biomedical entity matching to evaluate responses at the concept or disease level. More recently, GREEN [29] introduced a fine-grained factuality metric that explicitly identifies clinical findings and semantic errors by comparing generated and reference answers. Following [22], we employ GREEN to automatically assign hallucination labels to MLLM outputs, enabling the construction of a standardized benchmark for hallucination detection in medical VQA.

2.2. Hallucination Detection

Hallucination detection methods can be broadly divided into two categories: **collaborative** and **introspective** frameworks. **Collaborative approaches.** Collaborative methods rely on external models or knowledge sources to validate the correctness of generated responses. Some employ specialized *detector networks* [16, 30, 39] trained on curated hallucination datasets to distinguish factual from erroneous outputs. Others adopt *cross-model consistency* strategies [10, 41, 42], leveraging agreement among multiple LLMs or MLLMs to infer factual reliability. In addition, *visual evidence verification* frameworks [15, 33] integrate expert vision models to align textual claims with visual content. Although effective, these approaches require high-quality detectors or external supervision, constraining their scalability and adaptability across domains. **Introspective approaches.** Introspective methods eliminate external dependencies by enabling the MLLM to self-assess its factual consistency through internal reasoning or uncertainty estimation. Uncertainty-based methods [14, 21, 22] infer hallucinations by measuring predictive confidence or entropy, while *self-consistency analysis* [38, 42] evaluates semantic agreement across multiple reasoning paths. Despite their ef-

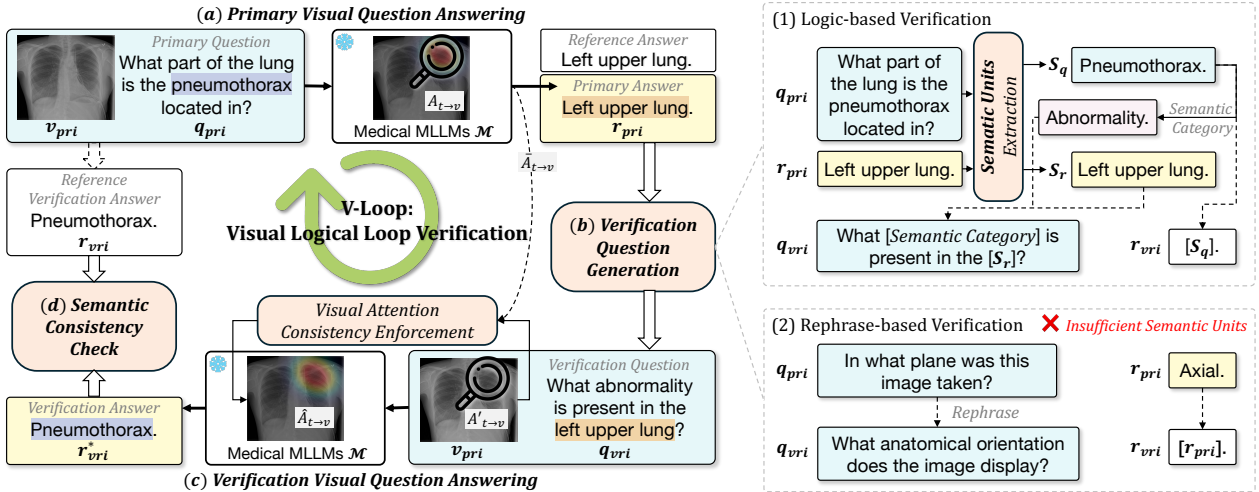


Figure 2. Overview of the proposed V-Loop framework. It consists of four stages, (a) primary visual question answering, where the MLLM generates the primary answer to the given image-question pair; (b) verification question generation, creating a verification question and its expected answer; (c) verification question answering, where the model answers the verification question under the same visual evidence; and (d) semantic consistency check, which evaluates the consistency between verification answer and its corresponding reference answer.

ficiency, these methods assess linguistic stability rather than factual grounding, and they do not verify whether a given answer aligns with visual evidence.

In contrast, our work introduces a visually grounded introspective framework that performs hallucination detection through a *bidirectional reasoning loop*. By enforcing both semantic and visual attention consistency, the proposed method achieves reliable hallucination verification in a training-free, plug-and-play manner.

3. Method

Given a medical image-question pair (q_{pri}, v_{pri}) , where q_{pri} seeks specific information from v_{pri} , a medical MLLM \mathcal{M} generates the response r_{pri} in an auto-regressive manner. To distinguish it from the verification question-answer pair discussed later, we refer to (q_{pri}, v_{pri}) as the primary question-answer pair and r_{pri} as the primary answer. Our objective is to detect whether r_{pri} contains hallucination.

3.1. Overview

As shown in Fig. 2, V-Loop proceeds in four compact steps: (1) *Primary VQA*: obtain $r_{pri} = \mathcal{M}(q_{pri}, v_{pri})$ and record the model’s text-to-image attention pattern during generation; (2) *Verification question generation (VQG)*: extract two semantic units from the primary triplet: \mathcal{S}_q (from q_{pri}) and \mathcal{S}_r (from r_{pri}), and produce a verification question q_{vri} and its reference answer r_{vri} using either logic-based inversion or rephrase-based equivalence; (3) *Verification VQA*: compute $r_{vri}^* = \mathcal{M}(q_{vri}, v_{pri})$ while enforcing visual attention consistency to ensure that reasoning uses the same image evidence as the primary stage; (4) *Semantic consistency check*: compare r_{vri}^* to r_{vri} with a deterministic semantic evaluator \mathcal{E} : disagreement indicates a broken loop and signals a hallucination. We now delve into the details.

3.2. Primary VQA

During Primary VQA, the medical MLLM \mathcal{M} generates a response r_{pri} based on the given image-question pair (q_{pri}, v_{pri}) . Then the concatenation of q_{pri} and r_{pri} forms a primary claim. For example, given the question ‘What part of the lung is the pneumothorax located in?’ and the answer ‘Left upper lung,’ the resulting claim becomes ‘The pneumothorax is located in the left upper lung.’ From the primary claim, we extract two compact **semantic units**: \mathcal{S}_q is extracted from q_{pri} , and \mathcal{S}_r is extracted from r_{pri} . Each semantic unit may represent a lesion, anatomical region, attribute, or other clinical concept, depending on the content of the primary pair. In the example above, \mathcal{S}_q is ‘pneumothorax’ and \mathcal{S}_r is ‘left upper lung’.

3.3. Verification Question Generation

Intuitively, the *verification question* is conditioned on the semantic unit \mathcal{S}_r extracted from the primary answer and is designed to re-query the semantic unit \mathcal{S}_q originating from the primary question. The expected verification answer is therefore the semantic unit \mathcal{S}_q itself, forming a semantic alignment between the primary and verification stages. Some question-answer pairs naturally contain two distinct semantic units, such as a queried entity and its contextual attribute, which enables the construction of a logical loop. However, others involve only a single semantic focus or lack a clear role exchange (e.g., ‘What imaging modality

is used?’ → ‘CT’), making such loop-based verification infeasible. To handle both cases effectively, we design two complementary strategies for verification question generation: (1) *logic-based verification*, which performs bidirectional reasoning consistency verification when dual semantic units are available, and (2) *rephrase-based verification*, which focuses on semantic equivalence checking when a logical loop cannot be formed.

Logic-based Verification. When both primary question and primary answer contain distinct semantic units S_q and S_r , we use S_r as the inquiry condition to re-query S_q during the verification stage. To enhance clarity and clinical relevance, S_q is further annotated with its *semantic category* (e.g., ‘Abnormality’, ‘Organ’, or ‘Attribute’), which provides the language model with explicit contextual guidance. This category-level supervision encourages the model to generate verification questions that are semantically precise, clinically grounded, and aligned with the original diagnostic intent. For example, when S_q (e.g., ‘pneumothorax’) is labeled as ‘Abnormality’, the model is prompted to generate domain-consistent questions such as ‘What abnormality is located in [region]?’ rather than a generic or ambiguous one like ‘What is located in [region]?’.

Rephrase-based verification. Not all primary question-answer pairs support the construction of a logic-based verification question. Suppose the pair lacks clear dual semantic units (single-focus queries such as modality, plane, or general image properties). In that case, we reformulate the primary question q_{pri} into a semantically equivalent question q_{vri} that preserves its intent while varying its linguistic structure, and then let the reference answer be the original one, *i.e.*, $r_{vri} = r_{pri}$. This reduces V-Loop to a semantic-equivalence check when logical inversion cannot be formed.

3.4. Verification VQA

In the verification stage, the generated verification question q_{vri} and the original image v_{pri} are fed into the MLLM \mathcal{M} to produce the verification answer r_{vri}^* . While this process mirrors the primary VQA stage, we introduce a **Visual Attention Consistency (VAC)** mechanism. This constraint ensures that the model performs verification based on the **same visual evidence** it relied upon when answering the primary question. Without this, the model might attend to unrelated image regions during the verification stage, leading to spurious results that are visually inconsistent with its original prediction. The VAC mechanism forces the MLLM to reuse the visual attention patterns from the primary answering stage, thereby maintaining consistent image-level evidence across both processes.

Attention aggregation. In the primary reasoning stage, let the attention map from the h -th head in the l -th layer be $A^{(l,h)}$. We isolate the text-to-image component, $A_{t \rightarrow v}^{(l,h)} \in \mathbb{R}^{N_t \times N_v}$, which captures the attention from text tokens

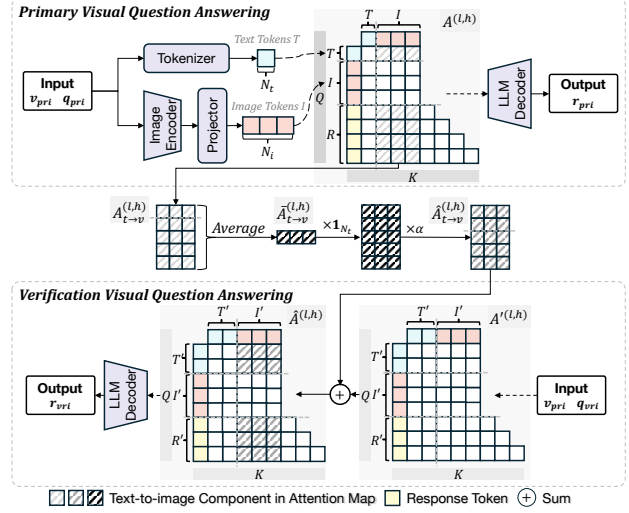


Figure 3. Visual Attention Consistency. The upper panel shows the primary stage, and the lower shows the verification process.

(originating from the primary question and its generated answer) to the N_v visual tokens. N_t is the number of text tokens. To create a global summary of visual focus, we average these text-to-image attention weights across all N_t text tokens, all H heads, and all L layers. This yields a single aggregated visual attention vector:

$$\bar{A}_{t \rightarrow v} = \frac{1}{LHN_t} \sum_{l=1}^L \sum_{h=1}^H \sum_{t=1}^{N_t} A_{t \rightarrow v}^{(l,h)} \in \mathbb{R}^{N_v}, \quad (1)$$

which represents the model’s overall attention pattern on image tokens from the primary reasoning stage.

Applying Aggregated Attention to Verification. In the backward verification stage, this aggregated visual pattern $\bar{A}_{t \rightarrow v}$ is utilized to regularize the verification attention. We first denote the attention map of the verification stage as $A'^{(l,h)}$, and scale $\bar{A}_{t \rightarrow v}$ by a coefficient α before injecting it into the text-to-image attention component $A'_{t \rightarrow v}^{(l,h)}$:

$$\hat{A}_{t \rightarrow v}^{(l,h)} = A'_{t \rightarrow v}^{(l,h)} + \alpha \times (\mathbf{1}_{N_t} \cdot \bar{A}_{t \rightarrow v}) \in \mathbb{R}^{N_t \times N_v}, \quad (2)$$

where $\mathbf{1}_{N_t} \in \mathbb{R}^{N_t \times 1}$ is an all-ones vector used to broadcast $\bar{A}_{t \rightarrow v}$ across all N_t text tokens.

The resulting reweighted block $\hat{A}_{t \rightarrow v}^{(l,h)}$ is substituted back into the full attention matrix $A'^{(l,h)}$, yielding the modified full matrix $\hat{A}^{(l,h)}$. To restore the probabilistic nature of the attention weights (which was disrupted by the addition), we apply a row-wise softmax operation to each row of $\hat{A}^{(l,h)}$. The normalized attention map $\tilde{A}^{(l,h)}$ is then used in the standard attention computation (*i.e.*, multiplied by the value matrix V) to produce the layer’s output. This VAC constraint guides the MLLM to perform verification using the same image evidence it relied upon during primary reasoning, thereby enforcing a visually grounded logical loop.

3.5. Semantic Consistency Check

We assess the semantic consistency between the generated verification answer r_{vri}^* and its reference answer r_{vri} . Note that the reference answer r_{vri} is defined as S_q for logic-based verification or r_{pri} for rephrase-based verification. This assessment determines whether the model forms a **logically closed reasoning loop**. If the two answers are semantically aligned, the primary claim is deemed grounded, indicating minimal hallucination risk. Conversely, a mismatch suggests the primary answer is hallucinated.

To assess this alignment, we utilize an auxiliary LLM, DeepSeek-V3.2-Exp [12], as a deterministic semantic evaluator, denoted as \mathcal{E} , to provide a reliable judgment. Given a pair (r_{vri}^*, r_{vri}) , the evaluator returns a similarity score $s \in [0, 1]$ measuring their semantic agreement:

$$s = \mathcal{E}(r_{vri}^*, r_{vri}). \quad (3)$$

A prediction is considered consistent only if $s = 1.0$. To ensure deterministic and reproducible outputs, this evaluation is conducted using a fixed prompt template with the evaluator’s generation temperature set to 0.0.

4. Experiments

4.1. Experimental Setup

Datasets. We evaluated *V-Loop* against competing hallucination detection methods on three medical VQA benchmarks that contain both closed-ended (binary ‘yes’/‘no’) and open-ended question-answer pairs: **VQA-RAD** [19] is a manually curated and clinically verified radiology VQA dataset comprising 2,244 QA pairs over 314 medical images. Its test set consists of 451 pairs from 203 images, including 200 open-ended and 251 closed-ended questions. **VQA-Med-2019** [1], introduced in the ImageCLEF 2019 VQA-Med challenge, contains 4,200 radiology images with 15,292 QA pairs. The test set includes 500 questions on 500 images across four categories, modality, plane, organ system, and abnormality, of which 436 are open-ended and 64 are closed-ended. **SLAKE** [25] is a semantically annotated bilingual dataset with 14,028 QA pairs over 642 images. We use the English portion of the test set (2,094 total, 645 open-ended / 416 closed-ended). All reported results include both the open-ended subset (most informative for hallucination diagnosis) and the full test set.

Backbones. We evaluated across two medical MLLMs and a general-purpose MLLM, which cover the common tradeoffs between medical specialization and model capacity. **MedGemma-4B-it** [34] is built upon the Gemma3 [36] architecture with a SigLIP-based visual encoder and is further aligned through large-scale medical image–text pre-training. **Lingshu-7B** [40] is a Qwen2.5-VL-based [4] multimodal model tailored for medical vision–language understanding through staged alignment and instruction tun-

ing. **InternVL3-8B** [45] follows the ‘ViT–MLP–LLM’ paradigm, integrating a Qwen2.5 series and InternLM3-8B language model with InternViT vision encoders and an MLP projector to bridge modalities.

Hallucination Detection Benchmark Construction.

Originally, the medical VQA datasets cannot be directly used to evaluate hallucination detection, as they provide neither the model-generated responses to be assessed nor the necessary hallucination labels. Following prior work [22], we (i) generated answers for every test sample using each evaluated MLLM and (ii) computed hallucination labels automatically via the **GREEN** model [29]. **GREEN** compares a generated answer to the reference, identifies matched findings and clinical errors, and returns

$$GREEN = \frac{\# \text{ matched findings}}{\# \text{ matched findings} + \# \text{ errors}}. \quad (4)$$

We treat samples with $GREEN < 1.0$ as containing hallucinations (label = 1.0) and $GREEN = 1.0$ as non-hallucinated (label = 0.0). This automatic evaluation pipeline facilitates scalable benchmarking of hallucination detection methods in line with recent practices.

Evaluation Metrics. Following prior hallucination detection studies [14, 22], we reported (1) the area under the ROC curve (AUC) and (2) the area under the **GREEN** Curve (AUG). **AUC** reflects the likelihood that a randomly chosen hallucinated response receives a higher detection score than a randomly chosen non-hallucinated one. For **AUG**, we first defined the *mean GREEN score at X%* as the average **GREEN** score of the top X% most confident samples, as ranked by each uncertainty-based method being evaluated. The **AUG** value is subsequently obtained by calculating the total area under the resulting confidence curve. This curve is formed by plotting the Mean **GREEN** score (y-axis) against X% (x-axis), by integrating over X ranging from 1% to 100% (with a 1% step size). This process effectively sums the mean scores across the entire confidence range. Larger **AUC** and **AUG** values consistently indicate a stronger hallucination detection capability.

Baselines. We compared our *V-Loop* framework against seven baselines, categorized by their approach to uncertainty estimation. Four baselines rely on MLLM’s output token probabilities. **AvgProb** [21] and **MaxProb** [21] measure model confidence by computing the average or maximum token probability of the generated sequence. **AvgEnt** [21] and **MaxEnt** [21] estimate model uncertainty by calculating the average or maximum entropy over the token-level probability distribution. Other baselines assess uncertainty by generating multiple responses. **SE** [14] estimates predictive uncertainty at the semantic level by generating multiple responses and computing the entropy of the semantic predictive distribution. **VASE** [22] further enhances **SE** by amplifying the influence of visual evidence during se-

Table 1. Performance (AUC (%)) and AUG (%) of V-Loop and seven competing methods. The best and second-best results are highlighted in **bold** and underline, respectively. * represents method which is uncertainty-based and requires additional K times response generation.

Method	VQA-RAD				VQA-Med-2019				SLAKE			
	Open-Ended		All		Open-Ended		All		Open-Ended		All	
	AUC	AUG										
MedGemma-4B-it [34]												
AvgProb [21]	36.36	43.47	44.49	54.25	42.96	35.43	44.41	38.33	44.02	58.77	43.01	56.26
AvgEnt [21]	<u>63.50</u>	60.17	55.60	58.33	<u>56.94</u>	32.85	55.42	35.40	55.98	60.72	56.98	57.20
MaxProb [21]	36.86	45.37	43.71	53.12	41.28	30.00	43.64	35.69	43.26	56.83	42.65	55.02
MaxEnt [21]	62.80	60.17	56.11	58.97	<u>58.58</u>	33.58	56.42	34.84	56.59	60.89	57.45	57.23
SE* [14]	63.33	<u>63.03</u>	56.65	<u>59.76</u>	61.88	<u>47.02</u>	60.91	48.78	<u>60.90</u>	<u>68.42</u>	56.84	<u>59.62</u>
RadFlag* [43]	62.91	62.87	<u>58.69</u>	57.94	<u>64.91</u>	36.42	<u>62.95</u>	<u>50.14</u>	59.18	63.57	59.56	58.53
Ours	66.32	66.51	60.30	66.91	66.02	50.92	63.28	52.15	61.87	68.60	59.31	65.15
Lingshu-7B [40]												
AvgProb [21]	50.52	47.85	48.27	56.36	45.93	<u>46.15</u>	45.64	<u>48.61</u>	46.87	70.07	46.75	69.97
AvgEnt [21]	49.48	47.07	<u>51.73</u>	<u>60.96</u>	54.07	39.98	54.36	41.31	53.13	74.38	<u>53.25</u>	<u>75.65</u>
MaxProb [21]	50.37	47.69	48.24	<u>55.44</u>	45.87	44.81	45.60	47.82	46.84	69.82	46.75	70.09
MaxEnt [21]	49.63	47.13	51.76	<u>60.96</u>	54.13	40.00	54.40	41.30	53.16	74.39	<u>53.25</u>	<u>75.65</u>
SE* [14]	<u>52.40</u>	<u>49.64</u>	50.96	59.16	51.80	39.39	51.90	38.72	50.58	73.61	50.89	75.61
RadFlag* [43]	51.90	48.35	51.55	59.29	<u>55.24</u>	40.67	<u>55.91</u>	42.77	<u>53.29</u>	<u>75.05</u>	52.52	75.44
Ours	70.00	56.47	50.04	62.84	71.93	66.33	65.66	65.03	67.68	84.01	59.79	81.83
InternVL3-8B [20]												
AvgProb [21]	39.88	42.12	39.77	43.33	38.89	33.64	39.74	37.45	41.62	46.91	41.24	46.19
AvgEnt [21]	58.89	51.44	59.67	54.34	60.46	42.05	60.17	47.90	58.47	54.34	58.09	55.58
MaxProb [21]	38.40	38.05	38.66	40.72	36.44	28.27	38.09	32.09	40.68	45.28	40.38	44.39
MaxEnt [21]	61.17	52.11	<u>61.59</u>	57.14	63.81	46.94	62.58	54.87	59.53	54.51	58.81	55.93
SE* [14]	61.26	53.89	60.04	56.01	66.18	52.19	66.35	46.71	58.24	54.03	<u>60.61</u>	<u>58.31</u>
RadFlag* [43]	<u>67.06</u>	<u>55.91</u>	63.99	57.98	<u>67.69</u>	<u>53.58</u>	<u>70.25</u>	<u>55.28</u>	64.93	58.76	62.12	59.75
Ours	68.20	57.68	60.98	58.15	72.86	56.58	70.55	55.82	<u>59.97</u>	59.77	56.04	57.96

mantic entropy estimation. RadFlag [43] is a consistency-based approach that quantifies the degree of agreement among multiple generated answers.

For the uncertainty-based methods (SE and RadFlag), the response generation time is set to 2. Please note that VASE estimates semantic entropy for both the original and perturbed images, resulting in a sampling frequency that is twice that of SE and RadFlag. Given its prohibitively high computational cost and to ensure a fair comparison, VASE is excluded from the main comparative experiments.

Implementation Details. Primary answers from all MLLMs were generated with decoding temperature $T = 0.1$. For sampling-based baselines (SE, RadFlag, VASE) we used $T = 1.0$ during the sampling stage. In V-Loop the verification answer is generated with $T = 0.1$. The attention reweighting coefficient is set to $\alpha = 0.7$ unless otherwise noted. All experiments were run on a single NVIDIA GeForce RTX 4090D GPU, and reported results are aggregated over the test splits described above.

Auxiliary LLM. VQG and semantic consistency check-

ing use an auxiliary text LLM in a text-only mode. Our primary choice is DeepSeek-V3.2-Exp [12] (zero sampling temperature for determinism). We also report results with GPT-4o [17] and Gemini-2.5-flash [11] for demonstrating the robustness of verification question generator choice in a controlled ablation (see Table 4).

4.2. Comparison Results

Table 1 reports AUC and AUG for all detection methods across datasets and model backbones. Generally, **V-Loop achieves the highest AUC/AUG scores** in the majority of settings, demonstrating particularly large gains on the **open-ended subsets**. The gains are smaller on the all splits because closed-ended samples often lack the dual semantic units required for logic-based verification. V-Loop therefore falls back to the weaker rephrase strategy, behaving more like standard consistency methods. Table 2 shows that integrating V-Loop consistently brings substantial gains across all uncertainty-based baselines (SE, RadFlag, and VASE) and all MLLMs. These improvements arise be-

Table 2. Performance (AUC (%)) and AUG (%) of uncertainty-based methods and their V-Loop-enhanced variants on VQA-Med-2019.

Method	Open-Ended		All		Open-Ended		All		Open-Ended		All	
	AUC	AUG	AUC	AUG	AUC	AUG	AUC	AUG	AUC	AUG	AUC	AUG
	MedGemma-4B-it [34]				Lingshu-7B [40]				InternVL3-8B [20]			
SE [14]	61.88	47.02	60.91	48.78	51.80	39.39	51.90	38.72	66.18	52.19	66.35	46.71
+ Ours	69.02	51.93	66.07	53.77	72.51	66.33	66.01	65.62	75.60	58.99	74.14	57.67
Δ	+7.14	+4.91	+5.16	+4.99	+20.71	+26.94	+14.11	+26.90	+9.42	+6.80	+7.79	+10.96
RadFlag [43]	64.91	36.42	62.95	50.14	55.24	40.67	55.91	42.77	67.69	53.58	70.25	55.28
+ Ours	71.11	53.89	67.02	53.91	73.42	66.43	67.23	65.22	76.14	58.23	75.92	60.79
Δ	+6.20	+17.47	+4.07	+3.77	+18.18	+25.76	+11.32	+22.45	+8.45	+4.65	+5.67	+5.51
VASE [22]	70.92	51.46	68.19	44.71	68.02	61.23	67.09	57.33	72.35	54.67	72.07	54.18
+ Ours	73.51	54.67	69.56	54.90	76.01	68.60	68.80	68.43	78.14	61.57	76.10	61.76
Δ	+2.59	+3.21	+1.37	+10.19	+7.99	+7.37	+1.71	+11.10	+5.79	+6.90	+4.03	+7.58

Table 3. Performance (AUC (%)) and AUG (%) of V-Loop and its variants on the open-ended splits of VQA-RAD and VQA-Med-2019 datasets with Lingshu-7B. VQG and VAC are the Verification Question Generation and Visual Attention Consistency Enforcement, respectively.

Components		VQA-RAD		VQA-Med-2019	
VQG	VAC	AUC	AUG	AUC	AUG
✗	✗	50.00	49.10	50.00	49.76
✗	✓	56.89↑	50.06↑	55.04↑	40.99↓
✓	✗	66.79↑	56.24↑	69.98↑	64.16↑
✓	✓	70.00↑	56.47↑	71.93↑	66.33↑

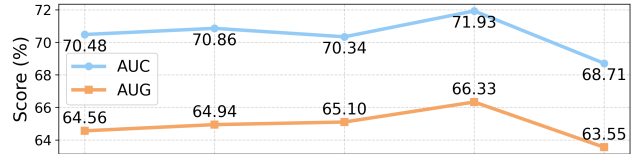


Figure 4. Effect of the weighting factor α on the performance (AUC (%)) and AUG (%) of V-Loop, evaluated on the VQA-RAD open-ended subset with MedGemma-4B-it.

cause uncertainty-based methods assess predictive uncertainty over the input pair, while V-Loop directly verifies the factual correctness of each specific answer. By combining global uncertainty cues with explicit answer-level verification, the enhanced variants deliver stronger and more reliable hallucination detection.

4.3. Ablation Study

Module ablation. We performed an ablation study to evaluate the contribution of two core components in V-Loop: VQG and VAC. We consider two ablated variants: (i) *w/o VQG*: the VQG module is removed and the original dataset

Table 4. Performance (AUC(%)) and AUG(%)) of V-Loop variants using different auxiliary LLMs for verification question generation on the VQA-RAD open-ended subset with Lingshu-7B.

Auxiliary LLM	AUC	AUG
DeepSeek-V3.2-Exp [12]	70.00	56.47
GPT-4o [28]	68.81	58.35
Gemini-2.5-Flash [11]	64.18	50.41

questions are reused as q_{vri} with the generation temperature being set to 1.0 to encourage response diversity; and (ii) *w/o VAC*: the visual attention consistency constraint is disabled during answering the verification question. The ablation results presented in Table 3 consistently show that removing either the VQG module or the VAC mechanism consistently degrades AUC and AUG, thereby confirming their essential and complementary roles. The VQG module materially improves the diagnostic power by providing semantically targeted verification questions that enable effective reasoning, while the VAC mechanism stabilizes the visual grounding during this process by enforcing the reuse of original visual evidence, which is crucial for reducing false positives. Overall, the complete V-Loop framework achieves the best results, highlighting their necessity for reliable, visually grounded hallucination detection.

Impact of LLM Quality on VQG. Table 4 examines the impact of using different auxiliary LLMs to generate verification questions. Across all settings, V-Loop consistently improves detection performance over the baseline, indicating that the framework is robust to the choice of auxiliary model. Stronger LLMs (e.g., DeepSeek-V3.2-Exp) yield larger gains, as they produce more accurate and clinically coherent verification questions, while smaller models (e.g., Gemini-2.5-Flash) still lead to substantial improvements. This shows that V-Loop is effective regardless of the auxiliary LLM used, and benefits further when higher-quality

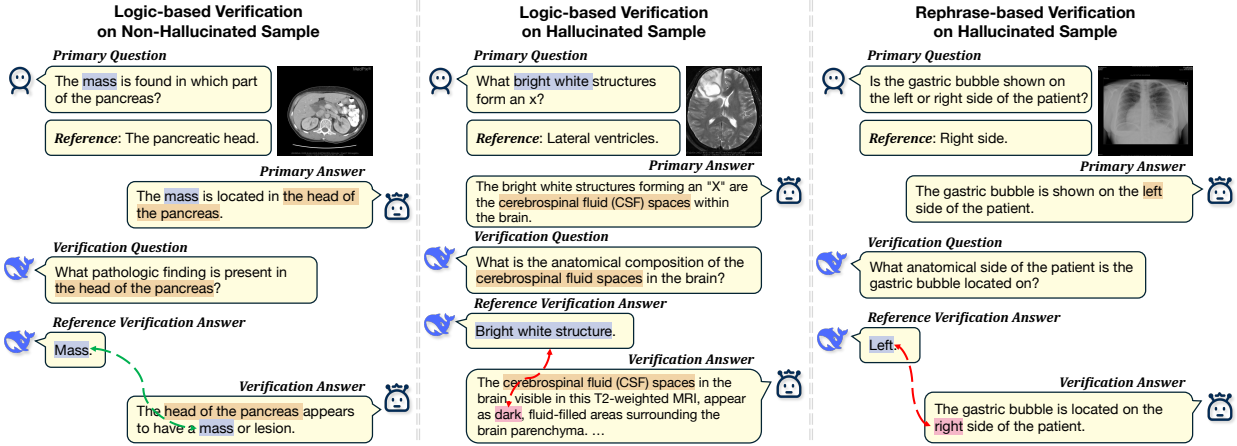
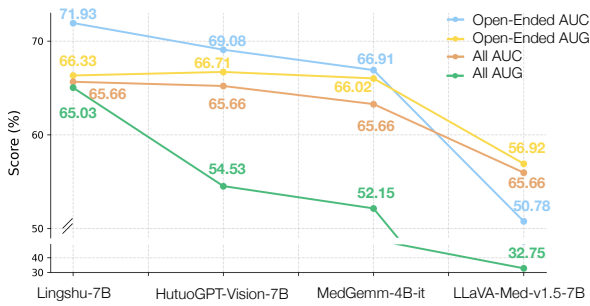
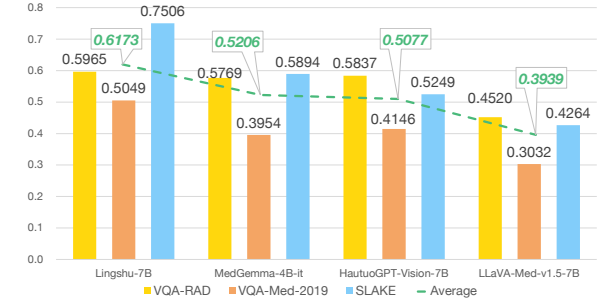


Figure 5. Examples of V-Loop. In each example, semantic units extracted from the question (blue) and answer (pink) are used to form the verification question. A correct verification answer closes the loop (left), while mismatches indicate hallucination (middle/right).



(a) Performance (AUC (%)) and AUG (%) of V-Loop on VQA-Med-2019 across medical MLLMs.



(b) Performance of medical MLLMs measured by the average GREEN score across all datasets.

Figure 6. Correlation between MLLM capability and V-Loop detection performance. Stronger models (higher GREEN scores) deliver higher AUC/AUG with V-Loop, highlighting its dependence on the MLLM’s visual–semantic reasoning quality.

verification questions are available.

Hyperparameter Selection. The weight factor α in Eq. 2 controls the strength of the visual attention consistency constraint by scaling the aggregated attention $\bar{A}_{t \rightarrow v}$. Fig. 4 presents the performance of V-Loop with different values of α on the VQA-RAD open-ended split. The proposed V-Loop framework maintains stable performance across a wide range of α values, demonstrating its robustness to parameter variation. The best results are achieved at $\alpha = 0.7$, where the model attains the optimal balance between maintaining visual grounding and allowing adaptive attention shifts during verification.

4.4. Impact of MLLM Competence

V-Loop relies on the underlying MLLM’s visual grounding and reasoning ability, making it sensitive to model quality. In Fig. 6a, V-Loop achieves notably lower AUC and AUG on weaker models such as LLaVA-Med-v1.5-7B [20]. To quantify this dependency, we compute each model’s av-

erage GREEN score across all datasets (Fig. 6b), where higher scores indicate stronger visual–semantic alignment. Models with low GREEN scores (e.g., LLaVA-Med-v1.5-7B) exhibit substantial hallucinations in both primary and verification stages, reducing V-Loop’s effectiveness, while stronger models (e.g., Lingshu-7B, MedGemm-4B-it) enable more accurate logical-loop verification.

5. Conclusion

In this paper, we presented V-Loop, a Visual Logical Loop Verification framework for hallucination detection in medical VQA. By constructing a verification question conditioned on the primary question–answer pair and constraining the model to answer it within the same visual region attended during the primary response, V-Loop enables the MLLM to detect hallucinated answers in a training-free, plug-and-play manner. Extensive experiments on multiple medical VQA benchmarks and MLLMs demonstrate that V-Loop outperforms other introspective detection methods and improves uncertainty-based methods when combined.

References

[1] Asma Ben Abacha, Sadid A Hasan, Vivek V Datla, Joey Liu, Dina Demner-Fushman, and Henning Müller. Vqa-med: Overview of the medical visual question answering task at imageclef 2019. *CLEF (working notes)*, 2(6):1–11, 2019. [5](#)

[2] Jean-Baptiste Alayrac, Jeff Donahue, Pauline Luc, Antoine Miech, Iain Barr, Yana Hasson, Karel Lenc, Arthur Mensch, Katherine Millican, Malcolm Reynolds, et al. Flamingo: a visual language model for few-shot learning. *Advances in neural information processing systems*, 35:23716–23736, 2022. [2](#)

[3] Asma Alkhaldi, Raneem Alnajim, Layan Alabdullatef, Rawan Alyahya, Jun Chen, Deyao Zhu, Ahmed Alsinan, and Mohamed Elhoseiny. Minigpt-med: Large language model as a general interface for radiology diagnosis. *arXiv preprint arXiv:2407.04106*, 2024. [2](#)

[4] Shuai Bai, Keqin Chen, Xuejing Liu, Jialin Wang, Wenbin Ge, Sibo Song, Kai Dang, Peng Wang, Shijie Wang, Jun Tang, et al. Qwen2. 5-vl technical report. *arXiv preprint arXiv:2502.13923*, 2025. [2, 5](#)

[5] Zechen Bai, Pichao Wang, Tianjun Xiao, Tong He, Zongbo Han, Zheng Zhang, and Mike Zheng Shou. Hallucination of multimodal large language models: A survey. *arXiv preprint arXiv:2404.18930*, 2024. [1](#)

[6] Liwei Che, Tony Qingze Liu, Jing Jia, Weiyi Qin, Ruixiang Tang, and Vladimir Pavlovic. Eazy: Eliminating hallucinations in lvmbs by zeroing out hallucinatory image tokens. *arXiv preprint arXiv:2503.07772*, 2025. [2](#)

[7] Junying Chen, Chi Gui, Ruyi Ouyang, Anningzhe Gao, Shunian Chen, Guiming Chen, Xidong Wang, Zhenyang Cai, Ke Ji, Xiang Wan, et al. Towards injecting medical visual knowledge into multimodal llms at scale. In *Proceedings of the 2024 Conference on Empirical Methods in Natural Language Processing*, pages 7346–7370, 2024. [1, 2](#)

[8] Jifan Chen, Grace Kim, Aniruddh Sriram, Greg Durrett, and Eunsol Choi. Complex claim verification with evidence retrieved in the wild. In *Proceedings of the 2024 Conference of the North American Chapter of the Association for Computational Linguistics: Human Language Technologies (Volume 1: Long Papers)*, pages 3569–3587, Mexico City, Mexico, 2024. Association for Computational Linguistics. [1](#)

[9] Zhihong Chen, Maya Varma, Jean-Benoit Delbrouck, Magdalini Paschali, Louis Blankemeier, Dave Van Veen, Jeya Maria Jose Valanarasu, Alaa Youssef, Joseph Paul Cohen, Eduardo Pontes Reis, et al. Chexagent: Towards a foundation model for chest x-ray interpretation. *arXiv preprint arXiv:2401.12208*, 2024. [1](#)

[10] Roi Cohen, May Hamri, Mor Geva, and Amir Globerson. Lm vs lm: Detecting factual errors via cross examination. In *Conference on Empirical Methods in Natural Language Processing*, 2023. [1, 2](#)

[11] Gheorghe Comanici, Eric Bieber, Mike Schaeckermann, Ice Pasupat, Noveen Sachdeva, Inderjit Dhillon, Marcel Blisstein, Ori Ram, Dan Zhang, Evan Rosen, et al. Gemini 2.5: Pushing the frontier with advanced reasoning, multimodality, long context, and next generation agentic capabilities. *arXiv preprint arXiv:2507.06261*, 2025. [6, 7](#)

[12] DeepSeek-AI. Deepseek-v3.2-exp: Boosting long-context efficiency with deepseek sparse attention, 2025. [5, 6, 7](#)

[13] Wenjie Dong, Shuhao Shen, Yuqiang Han, Tao Tan, Jian Wu, and Hongxia Xu. Generative models in medical visual question answering: A survey. *Applied Sciences*, 15(6):2983, 2025. [2](#)

[14] Sebastian Farquhar, Jannik Kossen, Lorenz Kuhn, and Yarin Gal. Detecting hallucinations in large language models using semantic entropy. *Nature*, 630(8017):625–630, 2024. [2, 5, 6, 7](#)

[15] Hao Fei, Meng Luo, Jundong Xu, Shengqiong Wu, Wei Ji, Mong-Li Lee, and Wynne Hsu. Fine-grained structural hallucination detection for unified visual comprehension and generation in multimodal llm. In *Proceedings of the 1st ACM Multimedia Workshop on Multi-Modal Misinformation Governance in the Era of Foundation Models*, page 13–22, New York, NY, USA, 2024. Association for Computing Machinery. [2](#)

[16] Romain Hardy, Sung Eun Kim, Du Hyun Ro, and Pranav Rajpurkar. Rextrust: A model for fine-grained hallucination detection in ai-generated radiology reports. In *Proceedings of The First AAAI Bridge Program on AI for Medicine and Healthcare*, pages 173–182. PMLR, 2025. [2](#)

[17] Aaron Hurst, Adam Lerer, Adam P Goucher, Adam Perelman, Aditya Ramesh, Aidan Clark, AJ Ostrow, Akila Welihinda, Alan Hayes, Alec Radford, et al. Gpt-4o system card. *arXiv preprint arXiv:2410.21276*, 2024. [6](#)

[18] Bidur Khanal, Sandesh Pokhrel, Sanjay Bhandari, Ramesh Rana, Nikesh Shrestha, Ram B. Gurung, Cristian Linte, Angus Watson, Yash R. Shrestha, and Binod Bhattacharai. Hallucination-Aware Multimodal Benchmark for Gastrointestinal Image Analysis with Large Vision-Language Models . In *proceedings of Medical Image Computing and Computer Assisted Intervention – MICCAI 2025*. Springer Nature Switzerland, 2025. [1](#)

[19] Jason J Lau, Soumya Gayen, Asma Ben Abacha, and Dina Demner-Fushman. A dataset of clinically generated visual questions and answers about radiology images. *Scientific data*, 5(1):1–10, 2018. [5](#)

[20] Chunyuan Li, Cliff Wong, Sheng Zhang, Naoto Usuyama, Haotian Liu, Jianwei Yang, Tristan Naumann, Hoifung Poon, and Jianfeng Gao. Llava-med: Training a large language-and-vision assistant for biomedicine in one day. *Advances in Neural Information Processing Systems*, 36:28541–28564, 2023. [1, 2, 6, 7, 8](#)

[21] Qing Li, Jiahui Geng, Chenyang Lyu, Derui Zhu, Maxim Panov, and Fakhri Karray. Reference-free hallucination detection for large vision-language models. In *Findings of the Association for Computational Linguistics: EMNLP 2024*, pages 4542–4551, Miami, Florida, USA, 2024. Association for Computational Linguistics. [2, 5, 6](#)

[22] Zehui Liao, Shishuai Hu, Ke Zou, Huazhu Fu, Liangli Zhen, and Yong Xia. Vision-amplified semantic entropy for hallucination detection in medical visual question answering. In *International Conference on Medical Image Computing and Computer-Assisted Intervention*. Springer, 2025. [2, 5, 7](#)

[23] Chin-Yew Lin. ROUGE: A package for automatic evaluation of summaries. In *Text Summarization Branches Out*, pages

74–81, Barcelona, Spain, 2004. Association for Computational Linguistics. 2

[24] Zhihong Lin, Donghao Zhang, Qingyi Tao, Danli Shi, Gholamreza Haffari, Qi Wu, Mingguang He, and Zongyuan Ge. Medical visual question answering: A survey. *Artificial Intelligence in Medicine*, 143:102611, 2023. 2

[25] Bo Liu, Li-Ming Zhan, Li Xu, Lin Ma, Yan Yang, and Xiao-Ming Wu. Slake: A semantically-labeled knowledge-enhanced dataset for medical visual question answering. In *2021 IEEE 18th international symposium on biomedical imaging (ISBI)*, pages 1650–1654. IEEE, 2021. 5

[26] Haotian Liu, Chunyuan Li, Qingsyang Wu, and Yong Jae Lee. Visual instruction tuning, 2023. 2

[27] Hanchao Liu, Wenyuan Xue, Yifei Chen, Dapeng Chen, Xiutian Zhao, Ke Wang, Liping Hou, Rongjun Li, and Wei Peng. A survey on hallucination in large vision-language models. *arXiv preprint arXiv:2402.00253*, 2024. 1

[28] Jacob Menick, Kevin Lu, Shengjia Zhao, E Wallace, H Ren, H Hu, N Stathas, and F Petroski Such. Gpt-4o mini: advancing cost-efficient intelligence. *Open AI: San Francisco, CA, USA*, 2024. 7

[29] Sophie Ostheimer, Justin Xu, Zhihong Chen, Maya Varma, Louis Blankemeier, Christian Bluethgen, Arne Edward Michalson Md, Michael Moseley, Curtis Langlotz, Akshay S Chaudhari, and Jean-Benoit Delbrouck. GREEN: Generative radiology report evaluation and error notation. In *Findings of the Association for Computational Linguistics: EMNLP 2024*, pages 374–390, Miami, Florida, USA, 2024. Association for Computational Linguistics. 2, 5

[30] Shrey Pandit, Ashwin Vinod, Liu Leqi, and Ying Ding. Teaching with lies: Curriculum dpo on synthetic negatives for hallucination detection. *arXiv preprint arXiv:2505.17558*, 2025. 2

[31] Kishore Papineni, Salim Roukos, Todd Ward, and Wei-Jing Zhu. Bleu: a method for automatic evaluation of machine translation. In *Proceedings of the 40th Annual Meeting of the Association for Computational Linguistics*, pages 311–318, Philadelphia, Pennsylvania, USA, 2002. Association for Computational Linguistics. 2

[32] Fuji Ren and Yangyang Zhou. Cgmvqa: A new classification and generative model for medical visual question answering. *IEEE Access*, 8:50626–50636, 2020. 2

[33] Pritish Sahu, Karan Sikka, and Ajay Divakaran. Pelican: Correcting hallucination in vision-LLMs via claim decomposition and program of thought verification. In *Proceedings of the 2024 Conference on Empirical Methods in Natural Language Processing*, pages 8228–8248, Miami, Florida, USA, 2024. Association for Computational Linguistics. 2

[34] Andrew Sellergren, Sahar Kazemzadeh, Tiam Jaroensri, Atilla Kiraly, Madeleine Traverse, Timo Kohlberger, Shawn Xu, Fayaz Jamil, Cian Hughes, Charles Lau, et al. Medgemma technical report. *arXiv preprint arXiv:2507.05201*, 2025. 1, 2, 5, 6, 7

[35] Bashar Talafha and Mahmoud Al-Ayyoub. Just at vqa-med: A vgg-seq2seq model. In *CLEF (working notes)*, 2018. 2

[36] Gemma Team, Aishwarya Kamath, Johan Ferret, Shreya Pathak, Nino Vieillard, Ramona Merhej, Sarah Perrin, Tatianna Matejovicova, Alexandre Ramé, Morgane Rivière, et al. Gemma 3 technical report. *arXiv preprint arXiv:2503.19786*, 2025. 5

[37] Jing Wu, Yunsoo Kim, and Honghan Wu. Hallucination benchmark in medical visual question answering. *arXiv preprint arXiv:2401.05827*, 2024. 1

[38] Junfei Wu, Qiang Liu, Ding Wang, Jinghao Zhang, Shu Wu, Liang Wang, and Tieniu Tan. Logical closed loop: Uncovering object hallucinations in large vision-language models. In *Findings of the Association for Computational Linguistics: ACL 2024*, pages 6944–6962, Bangkok, Thailand, 2024. Association for Computational Linguistics. 2

[39] Wenyi Xiao, Ziwei Huang, Leilei Gan, Wanggui He, Haoyuan Li, Zhenlin Yu, Fangxun Shu, Hao Jiang, and Linchao Zhu. Detecting and mitigating hallucination in large vision language models via fine-grained ai feedback. In *Proceedings of the AAAI Conference on Artificial Intelligence*, pages 25543–25551, 2025. 1, 2

[40] Weiwen Xu, Hou Pong Chan, Long Li, Mahani Aljunied, Ruiheng Yuan, Jianyu Wang, Chenghao Xiao, Guizhen Chen, Chaoqun Liu, Zhaodonghui Li, et al. Lingshu: A generalist foundation model for unified multimodal medical understanding and reasoning. *arXiv preprint arXiv:2506.07044*, 2025. 1, 2, 5, 6, 7

[41] Qifan Yu, Juncheng Li, Longhui Wei, Liang Pang, Wentao Ye, Bosheng Qin, Siliang Tang, Qi Tian, and Yueling Zhuang. Hallucidoctor: Mitigating hallucinatory toxicity in visual instruction data. In *Proceedings of the IEEE/CVF Conference on Computer Vision and Pattern Recognition*, pages 12944–12953, 2024. 2

[42] Jiaxin Zhang, Zhuohang Li, Kamalika Das, Bradley Malin, and Sricharan Kumar. SAC³: Reliable hallucination detection in black-box language models via semantic-aware cross-check consistency. In *Findings of the Association for Computational Linguistics: EMNLP 2023*, pages 15445–15458, Singapore, 2023. Association for Computational Linguistics. 2

[43] Serena Zhang, Sraavya Sambara, Oishi Banerjee, Julian N. Acosta, L. John Fahrner, and Pranav Rajpurkar. Radflag: A black-box hallucination detection method for medical vision language models. In *Proceedings of the 4th Machine Learning for Health Symposium*, pages 1087–1103. PMLR, 2025. 6, 7

[44] Tianyi Zhang*, Varsha Kishore*, Felix Wu*, Kilian Q. Weinberger, and Yoav Artzi. Bertscore: Evaluating text generation with bert. In *International Conference on Learning Representations*, 2020. 2

[45] Jinguo Zhu, Weiyun Wang, Zhe Chen, Zhaoyang Liu, Shenglong Ye, Lixin Gu, Hao Tian, Yuchen Duan, Weijie Su, Jie Shao, et al. Internvl3: Exploring advanced training and test-time recipes for open-source multimodal models. *arXiv preprint arXiv:2504.10479*, 2025. 2, 5

[46] Zhihong Zhu, Yunyan Zhang, Xianwei Zhuang, Fan Zhang, Zhongwei Wan, Yuyan Chen, QingqingLong QingqingLong, Yefeng Zheng, and Xian Wu. Can we trust ai doctors? a survey of medical hallucination in large language and large vision-language models. In *Findings of the Association for Computational Linguistics: ACL 2025*, pages 6748–6769, 2025. 1